Cure of Human Ovarian Carcinoma Solid Xenografts by Fractionated α-Radioimmunotherapy with ^{211}At-MX35-F(ab′)$_2$: Influence of Absorbed Tumor Dose and Effect on Long-Term Survival

Tom Bäck[1], Nicolas Chouin[2], Sture Lindegren[1], Helena Kahu[3], Holger Jensen[4], Per Albertsson[3], and Stig Palm[1]

[1]Department of Radiation Physics, Sahlgrenska Academy, University of Gothenburg, Gothenburg, Sweden; [2]LUNAM Université, Oniris, AMaROC, Nantes, France; [3]Department of Oncology, Sahlgrenska Academy, University of Gothenburg, Gothenburg, Sweden; and [4]PET and Cyclotron Unit, Department of Clinical Physiology and Nuclear Medicine, Copenhagen University Hospital, Copenhagen, Denmark

The goal of this study was to investigate whether targeted α-therapy can be used to successfully treat macrotumors, in addition to its established role for treating micrometastatic and minimal disease. We used an intravenous fractionated regimen of α-radioimmunotherapy in a subcutaneous tumor model in mice. We aimed to evaluate the absorbed dose levels required for tumor eradication and growth monitoring, as well as to evaluate long-term survival after treatment. **Methods:** Mice bearing subcutaneous tumors (50 mm^3, NIH:OVCAR-3) were injected repeatedly (1–3 intravenous injections 7–10 d apart, allowing bone marrow recovery) with ^{211}At-MX35-F(ab′)$_2$ at different activities (close to acute myelotoxicity). Mean absorbed doses to tumors and organs were estimated from biodistribution data and summed for the fractions. Tumor growth was monitored for 100 d and survival for 1 y after treatment. Toxicity analysis included body weight, white blood cell count, and hematocrit. **Results:** Effects on tumor growth after fractionated α-radioimmunotherapy with ^{211}At-MX35-F(ab′)$_2$ was strong and dose-dependent. Complete remission (tumor-free fraction, 100%) was found for tumor doses of 12.4 and 16.4 Gy. The administered activities were high, and long-term toxicity effects (≤60 wk) were clear. Above 1 MBq, the median survival decreased linearly with injected activity, from 44 to 11 wk. Toxicity was also seen by reduced body weight. White blood cell count analysis after α-radioimmunotherapy indicated bone marrow recovery for the low-activity groups, whereas for high-activity groups the reduction was close to acute myelotoxicity. A decrease in hematocrit was seen at a late interval (34–59 wk after therapy). The main external indication of poor health was dehydration. **Conclusion:** Having observed complete eradication of solid tumor xenografts, we conclude that targeted α-therapy regimens may stretch beyond the realm of micrometastatic disease and be eradicative also for macrotumors. Our observations indicate that at least 10 Gy are required. This agrees well with the calculated tumor control probability. Considering a relative biological effectiveness of 5, this dose level seems reasonable. However, complete remission was achieved first at activity levels close to lethal and was accompanied by biologic effects that reduced long-term survival.

Received May 16, 2016; revision accepted Sep. 8, 2016.

For correspondence or reprints contact: Tom Bäck, Department of Radiation Physics, University of Gothenburg, Gula Stråket 2B, SE-413 45 Gothenburg, Sweden.

E-mail: tom.back@radfys.gu.se

Published online Sep. 29, 2016.

Key Words: targeted alpha therapy; radioimmunotherapy; alpha-particles; ^{211}At; dosimetry

J Nucl Med 2017; 58:598–604
DOI: 10.2967/jnumed.116.178327

Radioimmunotherapy has long been seen as promising for various cancers, but its use in clinical practice has been limited. The main obstacle to greater success has been the tumor–to–normal tissue absorbed dose ratios, where only low or moderate levels have been reached, meaning that the activity amounts needed for tumor eradication could not be used because of the increased toxicity to normal tissue.

Most studies exploring radioimmunotherapy have used β-emitting radionuclides, but also α-particle–emitting radionuclides have been proposed, that is, α-radioimmunotherapy. α-particles have a much shorter range (50–100 μm) and higher linear energy transfer (~100 keV/μm) than β-particles, resulting in much higher tumor–to–normal tissue absorbed dose ratios for isolated single cancer cells or small cell clusters (*1*), such as micrometastases. α-emitters have therefore been studied, and proven successful experimentally, for therapy of microscopic tumors (*2–11*).

For irradiation of larger tumors, α-emitters do not have the same obvious advantages over β-emitters. Instead, the short path length of α-particles is likely a disadvantage. The antibody uptake in solid tumors has been shown to decrease with increasing tumor mass (*12*), such as because of elevated interstitial pressure, poor vascularization, and necrosis. In addition, the activity distribution within tumors is often heterogeneous because of poor diffusion of the antibody. The use of short-ranged α-emitters may therefore cause some fraction of the tumor cells to receive a very low absorbed dose. For the longer-ranged β-emitters, such as ^{90}Y, such obstacles might be partially compensated for by the cross-fire effect.

There may, however, be a rationale for using α-emitters in treatments also of macrotumors, such as when tumors can clinically be expected to occur at a spectrum of sizes ranging from single cells to millimeter-sized nodules. In addition to the favorable tumor–to–normal tissue absorbed dose ratios for microtumors, the radiobiologic effects of α-particles may make them favored over β-particles

also for solid tumors—for example, because of the induction of bystander effects (*13*). The need to use α-emitters in treatments of macrotumors may also arise with new regimens, such as pretargeted α-radioimmunotherapy (*14*), by which higher tumor–to–normal tissue absorbed dose ratios and more uniform tumor uptake can be achieved.

We have previously used ^{211}At-MX35-F(ab′)$_2$ in a subcutaneous macroscopic tumor model to derive the relative biological effectiveness (RBE) of α-radioimmunotherapy in vivo (*15*). Single intravenous administrations at different activities provided a range of absorbed doses to tumors, which were monitored for growth. The study showed a dose-dependent inhibition of growth, with the greatest delay seen for the highest tumor doses (2.7 and 4.1 Gy). However, all tumors resumed exponential growth, and the antitumor effect of a higher administered activity could not be evaluated because of bone marrow toxicity.

The aim of the present study was to investigate whether macrotumors can be eradicated by fractionated α-radioimmunotherapy and, if so, to determine the required absorbed tumor dose. The aim was also to evaluate the corresponding long-term toxicity. We used the subcutaneous tumor model, with 1–3 injections of ^{211}At-MX35 F(ab´)$_2$ administered 7–10 d apart. Tumor growth was monitored by volume measurements for up to 100 d, and long-term toxicity was monitored for up to 60 wk. Absorbed doses to tumors and normal tissues were calculated from previous biodistribution data, complemented by new data on the influence on tumor uptake from a prior α-radioimmunotherapy fraction.

MATERIALS AND METHODS

Radioimmunoconjugate

^{211}At (half-life, 7.2 h) was produced at the PET and Cyclotron Unit at Copenhagen University Hospital. The F(ab′)$_2$ fragment of the monoclonal antibody MX35 was produced by Strategic BioSolutions and kindly provided by the Memorial Sloan Kettering Cancer Center. The MX35 is directed to the sodium-dependent phosphate-transport protein 2b (NaPi2b) (*16*) expressed on about 90% of human epithelial ovarian cancers. Isolation of ^{211}At, radiolabeling, and immunoreactivity analysis were performed as previously described (*15,17,18*).

Tumor Model and Assessment of Therapy

The animals in the current study were also used in a previously published study assessing long-term renal toxicity after α-radioimmunotherapy (*19*). Using the human ovarian cancer cell line NIH: OVCAR-3 (obtained from American Type Culture Collection and cultured at 37°C in RPMI 1640 medium supplemented with 10% fetal calf serum, 2 mM L-glutamine, and 1% penicillin-streptomycin), 2 subcutaneous xenografts were established in the scapula region of each female nude mouse (BALB/c *nu/nu*, 4–8 wk old; Charles River) by inoculation of 2×10^7 cells (in 0.4 mL of phosphate-buffered saline).

At 6–12 d after cell inoculation (tumor volumes ~ 50 mm^3), α-radioimmunotherapy (^{211}At-MX35-F(ab′)$_2$; range, 0.36–1.53 MBq) was given by tail vein injection. Controls received unlabeled MX35-F(ab′)$_2$ only. Divided into 12 groups (8–10 animals per group), 4 groups received a single treatment, 8 groups received a second treatment after 7 d, and 4 groups also a third treatment, another 7 d later (Table 1).

The tumor volumes (V) were monitored by slide caliper measurements of the larger tumor diameter (D_L) and its perpendicular diameter (D_P), using the following formula (*20*): $V = (D_L \times D_P^2)/2$. When D_L exceeded 15 mm, or at signs of ulcerated skin, the tumors were surgically removed using isoflurane (Baxter Health Care Corp.) for anesthesia and Temgesic (RB Pharmaceuticals Limited) for sedation. After suture, the animals were monitored for recovery, and body temperature was assisted. Animals with tumor relapse were operated a second time. If they later presented with yet another relapse, they were removed from the study (and assigned as "censored" in the survival analysis).

Eighty days after tumor cell inoculation, the tumor-free fraction (TFF) was calculated by dividing the number of eradicated tumors by the initial number of tumors in each group. Tumors not viably established (volume < 25 mm^3) at first therapy were excluded from the analysis.

TABLE 1
Characteristics of Study Groups

Group	Mice (*n*)	Tumors (*n*)	Injection (MBq) 1	2	3	Total activity (MBq)	Median survival (wk)	Total absorbed tumor dose (Gy)	TFF
1	10	20	1.34	1.46	1.10	3.90	11	16.4	100%
2	10	20	0.87	0.63	0.77	2.27	28	9.5	45%
3	10	20	0.36	0.46	0.38	1.20	*N.D.*	5.0	5%
4	8	15	0.00	0.00	0.00	0.00	*N.D.*	0.0	0%
5	10	20	1.53	1.43	—	2.96	16	12.4	100%
6	10	20	1.02	0.60	—	1.62	40	6.8	20%
7	10	17	0.50	0.45	—	0.95	*N.D.*	4.0	42%
8	10	20	0.00	0.00	—	0.00	*N.D.*	0.0	0%
9	10	20	1.10	—	—	1.10	44	4.6	0%
10	10	20	0.77	—	—	0.77	*N.D.*	3.2	0%
11	10	20	0.38	—	—	0.38	*N.D.*	1.6	0%
12	10	20	0.00	—	—	0.00	*N.D.*	0.0	0%

TFF was calculated at 81–84 d after tumor inoculation for treated groups and at 39–41 d for control groups.

Blood sampled from the tail vein was analyzed for erythrocytes (hematocrit) and white blood cell (WBC) count. Hematocrit was monitored repeatedly over time. The WBC count was measured 5–7 d after α-radioimmunotherapy (representing nadir) and at 10–12 d (representing recovery). Blood samples (10 μL) from 3–5 animals per group were analyzed using a microcell counter (Sysmex F-820; Sysmex Corp.). Late-term WBC was analyzed in one animal per low-activity group (groups 6, 7, 9, 10 and 11) at 1 y (37–49 wk) after α-radioimmunotherapy.

Body weight and health status were monitored weekly until study termination (60 wk). The animals were sacrificed when showing signs of poor health, such as dehydration, abnormal behavior, or low weight progression. The study was approved by the local Ethics Committee, and all animals were maintained according to the regulations of the national Animal Welfare Agency.

Dosimetry

Mean absorbed dose to tumors and normal tissues was calculated from biodistribution data previously published for single ^{211}At-MX35-F(ab′)$_2$ administration (*15*). These data were complemented by a new biodistribution study to determine the uptake (percentage injected activity per gram) by tumors that had previously been treated with α-radioimmunotherapy. Nine tumor-carrying mice were administered 1.5 MBq of ^{211}At-MX35-F(ab′)$_2$, and 14 d later the biodistribution at 1, 9, and 21 h after injection (3 mice, i.e., 6 tumors per time point) after repeated α-radioimmunotherapy was determined.

Tissue activity concentrations at different times after injection were measured using a γ-counter (Wizard 1480; PerkinElmer Life Sciences), and the cumulated activity concentration, $\tilde{C}$ (total number of decays/kg), was calculated from time–activity plots up to 48 h after injection. The mean absorbed dose, *D,* was calculated from the formula

$$D = \tilde{C} \cdot \Delta \cdot \varnothing$$

using a mean α-particle energy (Δ) of 1.09×10^{-12} J per ^{211}At decay (neglecting contribution from photons and electrons) and an absorbed fraction, ∅, of 1.

Image-based small-scale 3-dimensional dosimetry was performed for one time point (4 h after injection) to evaluate the intratumoral activity and dose rate distribution using α-camera imaging (*21*) of serial tumor tissue sections and voxel dose-point kernels, as described before (*22,23*).

Statistical Analysis

Statistical differences were analyzed in Prism (GraphPad Software, Inc.) using the log-rank (Mantel–Cox) test for survival and linear regression for hematocrit.

RESULTS

Radioimmunoconjugate

After astatination, the immunoreactivity of the ^{211}At-MX35-F(ab′)$_2$ was 85%–95% and the radiochemical purity more than 95%.

Biodistribution and Dosimetry

The separate study investigating the potential influence on tumor uptake from prior α-radioimmunotherapy showed no difference in uptake between tumors previously treated or not (Supplemental Fig. 1; supplemental materials are available at http://jnm.snmjournals.org), and the values agreed well with those previously published (*15*). Hence, the tumor dose from repeated injections was calculated as the sum from all (1, 2, or 3) injections. The mean absorbed tumor dose was 4.2 Gy/MBq, and the total tumor doses for all study groups, shown in Table 1, ranged from 0 to 16.4 Gy. The mean absorbed doses for all organs are shown in Table 2.

Tumor Growth

The mean volume for all tumors at first treatment was 42 ± 28 (SD) mm^3. All treated mice had reduced tumor growth (Fig. 1) compared with the exponential growth of tumors on control mice. Groups receiving more than one fraction had the largest reduction. Overall, the tumor reduction was dose-dependent and initial reductions were followed by regrowth. In group 7 (Fig. 1B), 4 tumors were surgically removed on day 54 because of size, shifting the mean growth curve downward.

All tumors were eradicated in groups 1 and 5, which were treated with the highest total injected activity (3.90 and 2.96 MBq).

A TFF of 100% was found for tumor doses of 16.4 and 12.4 Gy, groups 1 and 5 (Table 1), respectively. At 9.5 Gy, group 2 had a TFF of 45%. A plot of TFF versus absorbed dose (Fig. 2) indicated a sigmoid dose response. For comparison, a theoretic calculation of tumor control probability (TCP) was done, using the mean tumor volume at therapy and previously observed data (*24*) on OVCAR-3 cell diameter (13.3 ± 2.2 μm) and sensitivity to α-irradiation (D_0) of 0.56 Gy. For higher dose levels, the experimental TFF agreed well with the theoretic TCP, whereas at lower dose levels the TFF was less steep, indicating biologic and dosimetric heterogeneity.

Blood

No obvious effect on hematocrit was seen at an early time interval (9–27 wk) after treatment, but at a late interval (34–59 wk)

TABLE 2
Absorbed Organ Doses

Organ	Mean absorbed dose (Gy/MBq)
Blood	5.0
Bone marrow*	2.0
Salivary glands	2.8
Throat	11
Thyroid†	45
Lung	3.4
Heart	2.0
Stomach	2.8
Small intestine	1.2
Large intestine	0.8
Liver	1.2
Spleen	1.5
Kidney	4.0
Intraperitoneal fat	0.8
Muscle	0.4
Tumor	4.2

*Dose to red bone marrow was estimated using marrow-to-blood ratio of 0.35.

†Dose to thyroid was estimated from throat content assuming that all activity was located in thyroid and using standard weight of 3 mg.

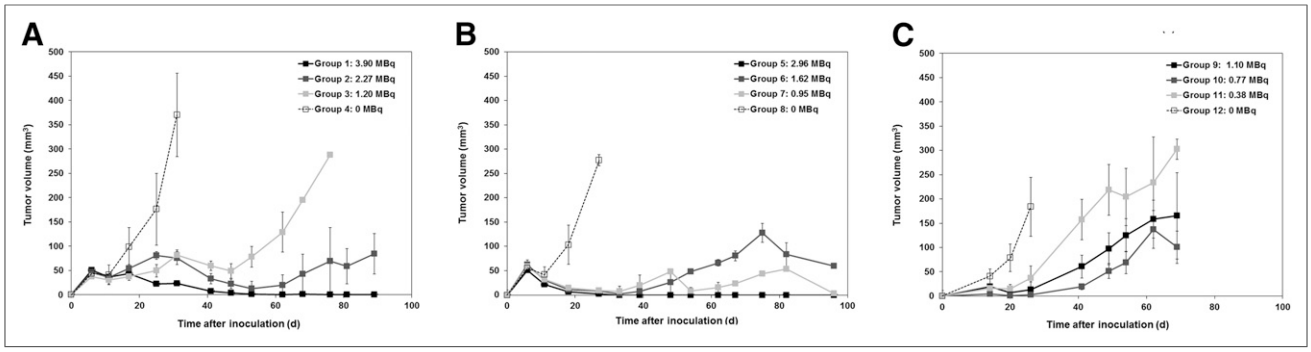

FIGURE 1. Mean tumor growth (±SEM) after intravenous fractionated α-radioimmunotherapy with ^{211}At-MX35-F(ab′)$_2$ plotted vs. time after first therapy: 3 fractions (A), 2 fractions (B), 1 fraction (C).

the mean values decreased linearly with increased activity (Fig. 3) and linear regression showed a slope significantly different from zero ($P = 0.0001$). Although the hematocrit for controls (groups 4, 8, and 12) were 57% ± 0.08%, 60% ± 0.08%, and 55% ± 0.04%, respectively, the groups treated with more than 1 MBq (3, 6, and 9) had values decreased to 50% ± 0.09%, 49% ± 0.06%, and 50% ± 0.04%, respectively. Group 2 (2.27 MBq) was the highest-activity group with late survivors, and the hematocrit value (44%) could be derived from only one mouse.

WBC count at 5–7 d after therapy was reduced to 70%–80% of the values for controls and then recovered. Ten to 12 d after the final α-radioimmunotherapy, the lower-activity groups (6, 7, 9, 10, and 11) had recovered to approximately 100%. Of these, one animal per group was used for long-term WBC counts, and 1 y (37–49 wk) after α-radioimmunotherapy their relative WBC count was 100% or more. In the higher-activity groups (1, 2, 3, and 5), WBC count had not recovered 10–12 d after the final administration and was 11%, 33%, 51%, and 65%, respectively. In these groups, late-term WBC count could not be analyzed.

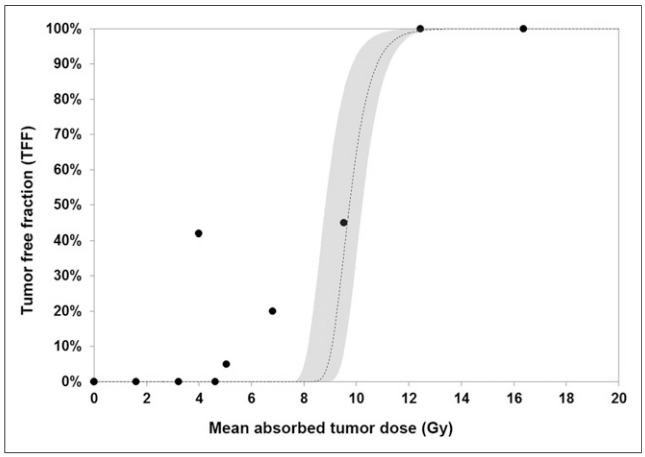

FIGURE 2. TFF plotted vs. mean absorbed tumor dose. Dashed curves represent theoretic TCP, calculated using mean tumor volume (42 ± 28 mm^3) and previously observed data (*24*) on OVCAR-3 cell diameter (13.3 ± 2.2 μm) and sensitivity to α-irradiation (D_0) of 0.56 Gy. Gray area indicates TCP range calculated from assuming two different numbers of cells in tumor using tumor volume (mean + SD) and cell diameter (mean − SD), or vice versa.

Body Weight

The weight progression for the highest-activity groups receiving multiple administrations (Figs. 4A and 4B) deviated from the controls relatively early (8–50 d). For groups receiving only one injection (Fig. 4 C), deviations from controls occurred later (~250 d). The lowest weight progression was seen for the highest-activity (3.90, 2.27, and 2.96 MBq) groups (1, 2, and 5, respectively), from which many animals had to be sacrificed shortly after α-radioimmunotherapy.

Survival

The impact on survival from systemic effects of α-radioimmunotherapy was studied after the tumors were either surgically removed at the maximum allowed volume or had been eradicated by repeated α-radioimmunotherapy. Survival was studied up to 60 wk (~400 d). A few animals had recurring tumor growth at the primary inoculation site after surgery. These were removed from the study and censored in the survival analysis.

Although undefined for most low-activity groups, the median survival (Table 1) for high-activity groups (above ~1 MBq) decreased linearly with increased total injected activity (Supplemental Fig. 2), from 44 wk for group 9 (1.10 MBq) down to 11 and 16 wk for groups 1 and 5 (3.90 and 2.96 MBq).

Figure 5 shows the Kaplan–Meier survival curves. For the groups receiving 3 fractions, statistical analysis by log-rank testing showed that groups 1 and 2, but not 3, were significantly different from their respective control (group 4). For the 2-fraction cohort, all treated groups were significantly different from the control (group 8), and for the 1-fraction cohort, only the group given the highest activity (group 9) was significantly different from the control.

DISCUSSION

We used a xenograft model to investigate the curative efficacy of fractionated systemic α-radioimmunotherapy on small, solid tumors. We showed that targeted α-therapy, although well suited for treatment of micrometastatic disease, could also eradicate small, solid tumor nodules. By use of fractionated α-radioimmunotherapy, high absorbed tumor doses were reached, accompanied by strong and dose-dependent antitumor effects. Complete remission (TFF, 100%) was found for tumor doses of 12.4 and 16.4 Gy. At 9.5 Gy, the TFF was 45%.

Most studies evaluating the antitumor efficacy of targeted α-therapy have used micrometastatic models, and tumor doses of 6–40 Gy have been reported for close to or complete remission

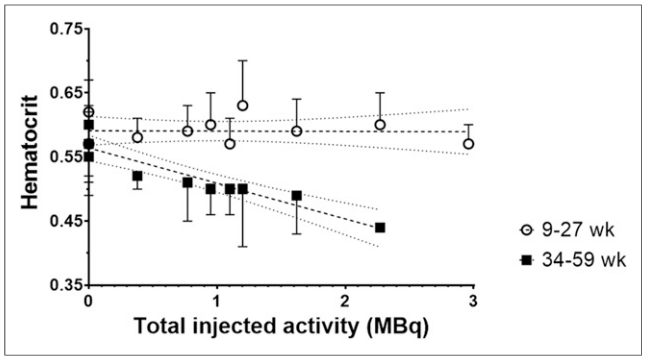

FIGURE 3. Hematocrit (mean ± SD) at early (○) and late (■) intervals after α-radioimmunotherapy injection, as function of total injected activity. Dashed lines indicate linear regression and 95% confidence interval.

(*2,7,25–28*). The therapeutic potential of α-emitters for macroscopic tumors has been sparsely investigated, and the dose levels required for tumor eradication are mostly unknown. A few studies have reported complete remission at absorbed doses of 12–21 Gy (*14,29,30*). Other studies reported antitumor effects that were close to, but not, curative (TFF, 60%–95%) for doses of 9–28 Gy (*31–37*). The dose levels found curative in the present study match these reported ones rather well. The biologic effects per unit dose for the densely ionizing α-particles are generally considerably greater than those for electrons and β-particles, and in the case of deterministic effects this difference can be accounted for by the use of RBE. We have chosen to report absorbed dose in units of grays, as recommended by the MIRD Committee (*38*). Assuming an RBE of 5 (*15*), our doses of 12.4 and 16.4 Gy would correspond to 62 and 82 Gy—that is, would agree well with the levels used in external-beam therapy.

In this study, the total absorbed tumor dose was calculated as the sum of the dose from each fraction. This could introduce errors since the tumor uptake could be altered from prior treatment, such as through increased vessel leakiness. However, when comparing untreated tumors with those previously treated, no difference in tumor uptake was observed (Supplemental Fig. 1). It could still be that the biologic response of the tumors was altered by prior therapy (i.e., a change in RBE), but the plot of TCP versus dose (Fig. 2) did not differ with the number of treatment factors. Therefore, the same absorbed dose factor (Gy/MBq) was used for all fractions. Although studies of biologic effects from α-particles would gain from a dosimetry more detailed than mean absorbed dose to whole organs in most cases, we chose to evaluate the antitumor effects with respect to mean absorbed dose to whole tumor. Using targeted α-therapy on solid tumors, antitumor effects may arise not only from irradiation of tumor cells but also from other targets, such as intratumoral vasculature (*25–27,39,40*). High-resolution α-camera imaging of the same tumor model as used here (*21*) showed clearly heterogeneous intratumoral activity distributions of up to 7 h after injection. Activity concentrations in stromal compartments were 5 times higher than the mean for the whole tumor, and total absorbed dose to stroma and near-stroma tumor cells was 2 times higher than for other cells (*41*). In the present study, imaging at 4 h after injection and initial 3-dimensional dosimetry (*22*) showed that some tumor areas had a dose rate 10 times higher than the mean (Fig. 6). The absorbed dose rate and its distribution has been shown to vary with time after injection in these macroscopic tumors (*21,22*) because of the temporal changes in intratumoral uptake and distribution. Besides the mean absorbed dose, the minimal absorbed tumor dose is of special interest and could be considered the limiting factor for antitumor efficacy. Preliminary data (*42*) from α-camera imaging at serial time points has shown that the minimal absorbed tumor dose was 30% lower than the mean. When comparing our TFF with a theoretic TCP, the experimental data disclosed a sigmoid, but shallower, dose–response curve (Fig. 2). Such a slope is generally interpreted to represent biologic and dosimetric heterogeneity and further supports the notion that the antitumor effects were not solely a question of dose effect in each tumor cell. This indicates that irradiation of vascular compartments may play an important role in targeted α-therapy of solid tumors and that improved methods for evaluating targeted α-therapy will likely involve small-scale dosimetry to these and other targets.

This study was designed to maximize tumor dose while avoiding acute bone marrow toxicity. The fraction scheme and activities were chosen to allow bone marrow recovery between fractions. However, the administered activities were high, and long-term toxicity effects (60 wk) were clear. The median survival decreased linearly with total injected activity from 59 to 11 wk. Toxicity was also seen by reduced body weight progression. WBC analysis after α-radioimmunotherapy indicated bone marrow recovery for low-activity groups, whereas for high-activity groups the reduction was close to acute myelotoxicity.

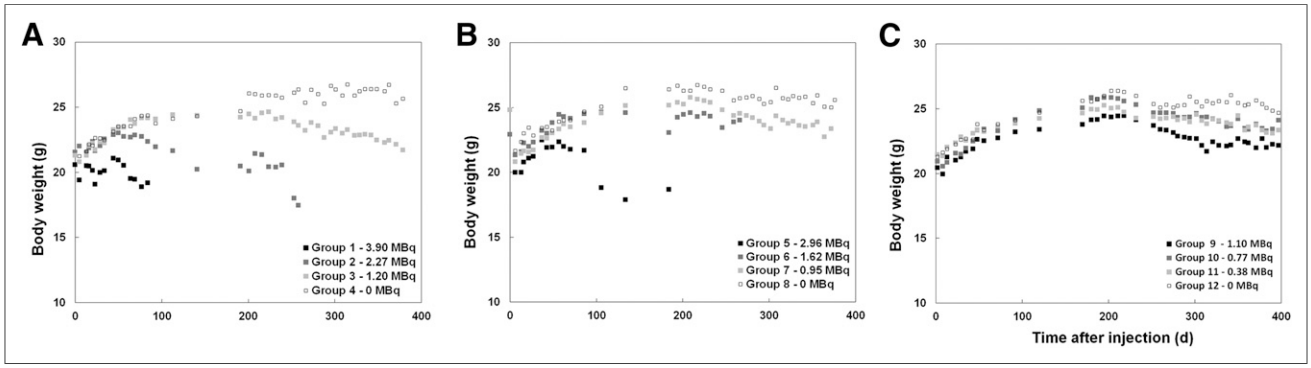

FIGURE 4. Mean body weights after first α-radioimmunotherapy injection in groups receiving 3 fractions (A), 2 fractions (B), and 1 fraction (C).

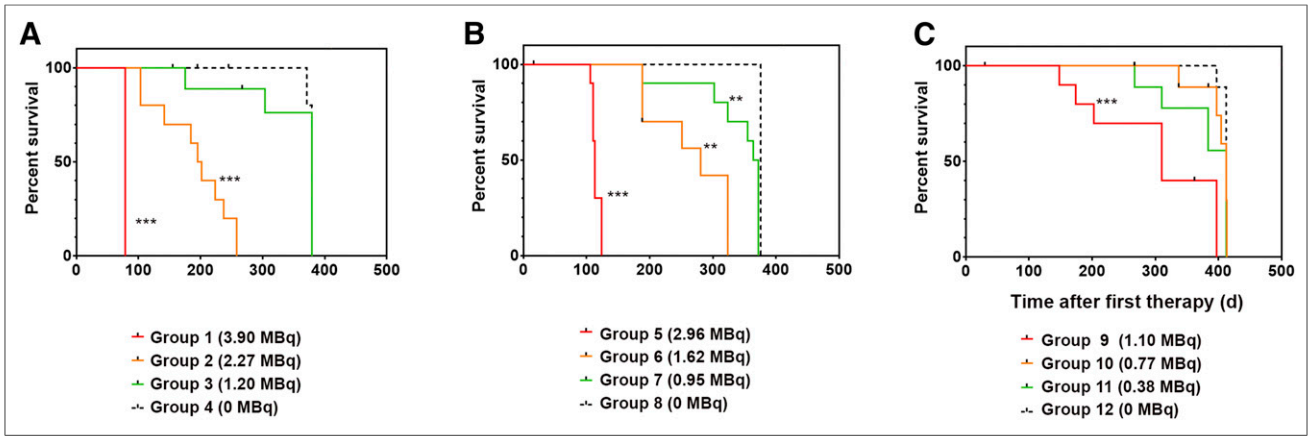

FIGURE 5. Percentage survival as function of time after first α-radioimmunotherapy injection: 3 fractions (A), 2 fractions (B), or 1 fraction (C). All tumors remaining after tumor growth monitoring period were surgically removed when exceeding 15 mm or at signs of ulcerated skin. Survival data therefore reflect other causes of death than progression of primary subcutaneous tumors, such as systemic radiotoxicity of α-radioimmunotherapy. If tumor regrowth occurred a third time after surgery, the animals were removed from the study and censored in survival analysis (tick marks). $^{**}P < 0.005$, treated vs. respective controls. $^{***}P < 0.0005$, treated vs. respective controls.

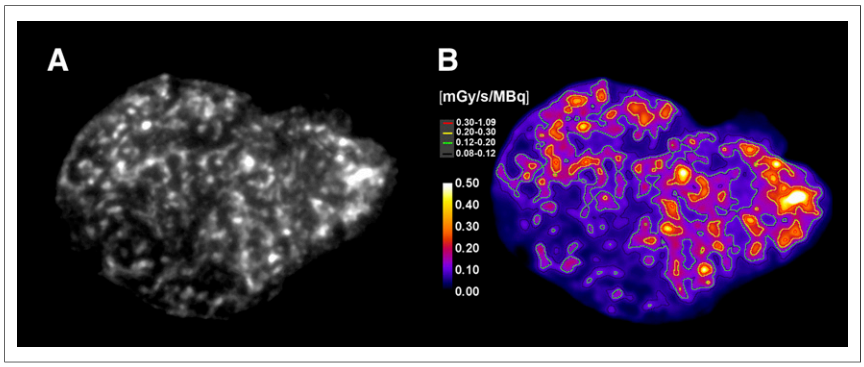

FIGURE 6. Intratumoral distribution on α-camera image of OVCAR-3 sc-tumor 4 h after injection after targeted α-therapy in mice with ^{211}At-MX35-F(Ab′)$_2$ (A) and dose rate image with isodose curves for intervals of 0.08–0.12 (black), 0.12–0.20 (green), 0.20–0.30 (yellow), and 0.30–1.09 (red) mGy/s/MBq (B).

A decrease in hematocrit was seen at a late interval (34–59 wk after therapy). The main external indication of poor health was dehydration and in some cases petechiae. We can only speculate on the reasons for reduced long-term survival, but since we observed a linear decrease in median survival with increasing injected activity, we interpret the effects on survival as being due to systemic radiotoxicity. Although myelotoxicity is a potential cause, as indicated by the WBC and hematocrit data, several organs had an absorbed dose above (bone marrow, thyroid, throat, lungs and kidneys) or close to (stomach, heart) their tolerance dose (calculated for 3 MBq and assuming an RBE of 5 for α-irradiation). We have initiated further studies to gain more knowledge of long-term toxicity after targeted α-therapy regimens.

Although targeted α-therapy may be most promising for treatment of minimal disease, our findings show that α-emitters might prove useful also for solid tumors, provided that the normal tissue toxicity can be kept at acceptable levels. This may have clinical importance, since many of the patients recruited for targeted α-therapy of minimal disease will likely have tumor sizes ranging from single cells to small, solid nodules. Further improvements will likely involve new treatment modalities by which normal-tissue toxicity might be reduced, as indicated for pretargeted α-radioimmunotherapy (*14,34*). A prerequisite for any treatment planning will, however, involve knowledge of the absorbed doses required for tumor eradication. With all the limitations for translating results derived experimentally in an animal model to humans, the results from the current study support further exploration of targeted α-therapy for treating solid tumors.

CONCLUSION

We investigated whether targeted α-therapy, in addition to its promising role for treating micrometastatic and minimal disease, can also be used to treat macrotumors. Using intravenous fractionated α-radioimmunotherapy, we found eradication of solid tumor xenografts receiving absorbed doses of 12.4 and 16.4 Gy. Hence, we conclude that targeted α-therapy regimens can stretch beyond the realm of micrometastatic disease and be eradicative also for solid tumors. Our observations indicate that at least 10 Gy are required, and this experimental finding agrees well with theoretic calculations of TCP. Considering an RBE of 5, this dose level seems reasonable. However, complete remission was achieved first at activity levels close to lethal and was accompanied by biologic effects that reduced long-term survival.

DISCLOSURE

This work was supported by the Swedish Research Council, the Swedish Cancer Society, the King Gustaf V Jubilee Clinic Cancer Research Foundation, and the Assar Gabrielsson Cancer Research Foundation. No other potential conflict of interest relevant to this article was reported.

REFERENCES

1. Uusijärvi H, Bernhardt P, Ericsson T, Forssell-Aronsson E. Dosimetric characterization of radionuclides for systemic tumor therapy: influence of particle range, photon emission, and subcellular distribution. *Med Phys.* 2006;33:3260–3269.
2. Kennel SJ, Mirzadeh S. Vascular targeted radioimmunotherapy with ^{213}Bi: an alpha-particle emitter. *Nucl Med Biol.* 1998;25:241–246.
3. Allen BJ, Tian Z, Rizvi SM, Li Y, Ranson M. Preclinical studies of targeted alpha therapy for breast cancer using ^{213}Bi-labelled-plasminogen activator inhibitor type 2. *Br J Cancer.* 2003;88:944–950.
4. Michel RB, Rosario AV, Brechbiel MW, Jackson TJ, Goldenberg DM, Mattes MJ. Experimental therapy of disseminated B-cell lymphoma xenografts with ^{213}Bi-labeled anti-CD74. *Nucl Med Biol.* 2003;30:715–723.
5. Qu CF, Songl YJ, Rizvi SM, et al. In vivo and in vitro inhibition of pancreatic cancer growth by targeted alpha therapy using ^{213}Bi-CHX.A″-C595. *Cancer Biol Ther.* 2005;4:848–853.
6. Beck R, Seidl C, Pfost B, et al. ^{213}Bi-radioimmunotherapy defeats early-stage disseminated gastric cancer in nude mice. *Cancer Sci.* 2007;98:1215–1222.
7. Song H, Shahverdi K, Huso DL, et al. ^{213}Bi (alpha-emitter)-antibody targeting of breast cancer metastases in the neu-N transgenic mouse model. *Cancer Res.* 2008;68:3873–3880.
8. Borchardt PE, Yuan RR, Miederer M, McDevitt MR, Scheinberg DA. Targeted actinium-225 in vivo generators for therapy of ovarian cancer. *Cancer Res.* 2003;63:5084–5090.
9. Andersson H, Elgqvist J, Horvath G, et al. Astatine-211-labeled antibodies for treatment of disseminated ovarian cancer: an overview of results in an ovarian tumor model. *Clin Cancer Res.* 2003;9(suppl):3914S–3921S.
10. Elgqvist J, Andersson H, Back T, et al. Alpha-radioimmunotherapy of intraperitoneally growing OVCAR-3 tumors of variable dimensions: outcome related to measured tumor size and mean absorbed dose. *J Nucl Med.* 2006;47:1342–1350.
11. Gustafsson AM, Back T, Elgqvist J, et al. Comparison of therapeutic efficacy and biodistribution of ^{213}Bi- and ^{211}At-labeled monoclonal antibody MX35 in an ovarian cancer model. *Nucl Med Biol.* 2012;39:15–22.
12. Hagan PL, Halpern SE, Dillman RO, et al. Tumor size: effect on monoclonal antibody uptake in tumor models. *J Nucl Med.* 1986;27:422–427.
13. Wang R, Coderre JA. A bystander effect in alpha-particle irradiations of human prostate tumor cells. *Radiat Res.* 2005;164:711–722.
14. Park SI, Shenoi J, Pagel JM, et al. Conventional and pretargeted radioimmunotherapy using bismuth-213 to target and treat non-Hodgkin lymphomas expressing CD20: a preclinical model toward optimal consolidation therapy to eradicate minimal residual disease. *Blood.* 2010;116:4231–4239.
15. Bäck T, Andersson H, Divgi CR, et al. ^{211}At radioimmunotherapy of subcutaneous human ovarian cancer xenografts: evaluation of relative biologic effectiveness of an alpha-emitter in vivo. *J Nucl Med.* 2005;46:2061–2067.
16. Yin BW, Kiyamova R, Chua R, et al. Monoclonal antibody MX35 detects the membrane transporter NaPi2b (SLC34A2) in human carcinomas. *Cancer Immun.* 2008;8:3.
17. Lindegren S, Back T, Jensen HJ. Dry-distillation of astatine-211 from irradiated bismuth targets: a time-saving procedure with high recovery yields. *Appl Radiat Isot.* 2001;55:157–160.
18. Lindegren S, Frost S, Back T, Haglund E, Elgqvist J, Jensen H. Direct procedure for the production of ^{211}At-labeled antibodies with an epsilon-lysyl-3-(trimethylstannyl)benzamide immunoconjugate. *J Nucl Med.* 2008;49:1537–1545.
19. Bäck T, Haraldsson B, Hultborn R, et al. Glomerular filtration rate after alpha-radioimmunotherapy with ^{211}At-MX35-F(ab′)2: a long-term study of renal function in nude mice. *Cancer Biother Radiopharm.* 2009;24:649–658.
20. Carlsson G, Gullberg B, Hafstrom L. Estimation of liver tumor volume using different formulas: an experimental study in rats. *J Cancer Res Clin Oncol.* 1983;105:20–23.
21. Bäck T, Jacobsson L. The alpha-camera: a quantitative digital autoradiography technique using a charge-coupled device for ex vivo high-resolution bioimaging of alpha-particles. *J Nucl Med.* 2010;51:1616–1623.
22. Bäck T, Chouin N, Lindegren S, Jensen H, Albertsson P, Palm S. Image-based small-scale 3D-dosimetry in targeted alpha therapy using voxel dose-point kernels and alpha camera imaging of serial tissue sections [abstract]. *J Nucl Med.* 2014;55(suppl):50.
23. Frost SH, Miller BW, Back TA, et al. Alpha-imaging confirmed efficient targeting of CD45-positive cells after ^{211}At-radioimmunotherapy for hematopoietic cell transplantation. *J Nucl Med.* 2015;56:1766–1773.
24. Palm S, Andersson H, Back T, et al. In vitro effects of free ^{211}At,^{211}At-albumin and ^{211}At-monoclonal antibody compared to external photon irradiation on two human cancer cell lines. *Anticancer Res.* 2000;20:1005–1012.
25. Kennel SJ, Boll R, Stabin M, Schuller HM, Mirzadeh S. Radioimmunotherapy of micrometastases in lung with vascular targeted ^{213}Bi. *Br J Cancer.* 1999;80:175–184.
26. Kennel SJ, Chappell LL, Dadachova K, et al. Evaluation of ^{225}Ac for vascular targeted radioimmunotherapy of lung tumors. *Cancer Biother Radiopharm.* 2000;15:235–244.
27. Kennel SJ, Mirzadeh S, Eckelman WC, et al. Vascular-targeted radioimmunotherapy with the alpha-particle emitter ^{211}At. *Radiat Res.* 2002;157:633–641.
28. Song H, Hobbs RF, Vajravelu R, et al. Radioimmunotherapy of breast cancer metastases with alpha-particle emitter ^{225}Ac: comparing efficacy with ^{213}Bi and ^{90}Y. *Cancer Res.* 2009;69:8941–8948.
29. Petrich T, Quintanilla-Martinez L, Korkmaz Z, et al. Effective cancer therapy with the alpha-particle emitter [^{211}At]astatine in a mouse model of genetically modified sodium/iodide symporter-expressing tumors. *Clin Cancer Res.* 2006;12:1342–1348.
30. Petrich T, Helmeke HJ, Meyer GJ, Knapp WH, Potter E. Establishment of radioactive astatine and iodine uptake in cancer cell lines expressing the human sodium/iodide symporter. *Eur J Nucl Med Mol Imaging.* 2002;29:842–854.
31. Behr TM, Behe M, Stabin MG, et al. High-linear energy transfer (LET) alpha versus low-LET beta emitters in radioimmunotherapy of solid tumors: therapeutic efficacy and dose-limiting toxicity of ^{213}Bi- versus ^{90}Y-labeled CO17-1A Fab′ fragments in a human colonic cancer model. *Cancer Res.* 1999;59:2635–2643.
32. Norenberg JP. ^{213}Bi-DOTA-octreotide peptide receptor radionuclide therapy of pancreatic tumors in a preclinical animal model. Presented at: 8th International Symposium on Targeted Alpha Therapy; 2013; Oak Ridge, Tennessee.
33. Norenberg JP, Krenning BJ, Konings IR, et al. ^{213}Bi-[DOTA0, Tyr3]octreotide peptide receptor radionuclide therapy of pancreatic tumors in a preclinical animal model. *Clin Cancer Res.* 2006;12:897–903.
34. Pagel JM, Kenoyer AL, Back T, et al. Anti-CD45 pretargeted radioimmunotherapy using bismuth-213: high rates of complete remission and long-term survival in a mouse myeloid leukemia xenograft model. *Blood.* 2011;118:703–711.
35. Wild D, Frischknecht M, Zhang H, et al. Alpha- versus beta-particle radiopeptide therapy in a human prostate cancer model (^{213}Bi-DOTA-PESIN and ^{213}Bi-AMBA versus ^{177}Lu-DOTA-PESIN). *Cancer Res.* 2011;71:1009–1018.
36. Dahle J, Bruland OS, Larsen RH. Relative biologic effects of low-dose-rate alpha-emitting ^{227}Th-rituximab and beta-emitting ^{90}Y-tiuexetan-ibritumomab versus external beam x-radiation. *Int J Radiat Oncol Biol Phys.* 2008;72:186–192.
37. Dahle J, Borrebaek J, Jonasdottir TJ, et al. Targeted cancer therapy with a novel low-dose rate alpha-emitting radioimmunoconjugate. *Blood.* 2007;110:2049–2056.
38. Sgouros G, Roeske JC, McDevitt MR, et al. MIRD pamphlet no. 22 (abridged): radiobiology and dosimetry of alpha-particle emitters for targeted radionuclide therapy. *J Nucl Med.* 2010;51:311–328.
39. Behling K, Maguire WF, López Puebla JC, et al. Vascular targeted radioimmunotherapy for the treatment of glioblastoma. *J Nucl Med.* 2016;57:1576–1582.
40. Singh Jaggi J, Henke E, Seshan SV, et al. Selective alpha-particle mediated depletion of tumor vasculature with vascular normalization. *PLoS One.* 2007;2:e267.
41. Chouin N, Back T, Bardies M, et al. Statistical and dosimetric analysis of the penetration of antibody fragments F(ab′)2 radiolabeled with ^{211}At within subcutaneous tumors [abstract]. *J Nucl Med.* 2011;52(suppl):75.
42. Chouin N, Palm S, Lindegren S, Jensen H, Albertsson P, Back T. Intra-tumoral dose distributions after experimental targeted alpha therapy by alpha-camera imaging. *Eur J Nucl Med Mol Imaging.* 2014;41:151–705.